C. R. Chimie 5 (2002) 111–118
© 2002 Académie des sciences/Éditions scientifiques et médicales Elsevier SAS. Tous droits réservés
S1631074802013516/FLA

An unexpected insertion of acetone into the silicon–carbon terminus of an sp carbon chain: syntheses and structures of model monoplatinum hexatriynyl and octatetraynyl complexes

Wolfgang Mohr[a], Thomas B. Peters[b], James C. Bohling[b], Frank Hampel[a], Atta M. Arif[b], John A. Gladysz[a]*

[a] *Institut für Organische Chemie, Friedrich-Alexander Universität Erlangen-Nürnberg, Henkestrasse 42, 91054 Erlangen, Germany*
[b] *Department of Chemistry, University of Utah, Salt Lake City, Utah 84112, USA*

Received 11 July 2001; accepted 23 October 2001

Abstract – The sequential treatment of *trans*-$(C_6F_5)(p\text{-tol}_3P)_2PtC{\equiv}CC{\equiv}CC{\equiv}CSiEt_3$ (**2**, acetone solution) with $n\text{-}Bu_4N^+ F^-$ in wet THF (to generate a $PtC{\equiv}CC{\equiv}CC{\equiv}CH$ complex), $ClSiMe_3$ (fluoride ion scavenger), excess $HC{\equiv}CSiEt_3$, excess O_2, and CuCl/TMEDA (0.20–0.25 equiv in acetone; Hay cross-coupling conditions) gives *trans*-$(C_6F_5)(p\text{-tol}_3P)_2PtC{\equiv}CC{\equiv}CC{\equiv}CC{\equiv}CSiEt_3$ (**4**, 30%), as previously reported. When an analogous reaction is conducted with $SiMe_4$ in place of $ClSiMe_3$, the side-product *trans*-$(C_6F_5)(p\text{-tol}_3P)_2PtC{\equiv}CC{\equiv}CC{\equiv}CC(Me)_2OSiEt_3$ is obtained (ca 28%), the structure of which is established crystallographically. For comparison, crystal structures of three related complexes, **4**, **2**, and *trans*-$(p\text{-tol})(Ph_3P)_2PtC{\equiv}CC{\equiv}CC{\equiv}CSiEt_3$, are determined. ***To cite this article: W. Mohr et al., C. R. Chimie 5 (2002) 111–118*** © 2002 Académie des sciences/Éditions scientifiques et médicales Elsevier SAS

platinum / alkynyl complexes / Hay coupling / crystal structures

Résumé – Le traitement successif de *trans*-$(C_6F_5)(p\text{-tol}_3P)_2PtC{\equiv}CC{\equiv}CC{\equiv}CSiEt_3$ (**2**, en solution dans l'acétone) par une solution de $n\text{-}Bu_4N^+ F^-$ dans du THF non séché (pour générer le complexe $PtC{\equiv}CC{\equiv}CC{\equiv}CH$), puis par $ClSiMe_3$ (pour piéger les ions fluorure), enfin par un excès de $HC{\equiv}CSiEt_3$, un excès de O_2 en présence de CuCl/TMEDA (0,20–0,25 equiv en solution dans l'acétone ; conditions de réaction de couplage croisé de Hay) conduit au complexe *trans*-$(C_6F_5)(p\text{-tol}_3P)_2PtC{\equiv}CC{\equiv}CC{\equiv}CC{\equiv}CSiEt_3$ (**4**, 30%), comme précédemment rapporté. Quand la réaction est conduite de façon similaire avec $SiMe_4$ à la place de $ClSiMe_3$, le produit secondaire *trans*-$(C_6F_5)(p\text{-tol}_3P)_2PtC{\equiv}CC{\equiv}CC{\equiv}CC(Me)_2OSiEt_3$ est obtenu (ca 28%). La structure de ce composé a été établie par radiocristallographie et comparée à celles des complexes **4**, **2** et *trans*-$(p\text{-tol})(Ph_3P)_2PtC{\equiv}CC{\equiv}CC{\equiv}CSiEt_3$, également déterminées. ***Pour citer cet article : W. Mohr et al., C. R. Chimie 5 (2002) 111–118*** © 2002 Académie des sciences/Éditions scientifiques et médicales Elsevier SAS

platine / complexes alkynyle / couplage croisé de Hay / structures cristallines

* *Correspondence and reprints.*
E-mail address: gladysz@organik.uni-erlangen.de (J.A. Gladysz).

1. Introduction

This thematic issue of *Comptes Rendus* celebrates a GECOM–CONCOORD Symposium held in Albé (Alsace) 13–18 May 2001. Our oral presentation described a variety of developments involving complexes in which sp carbon chains span two transition metals, **I**, a good background for which is available in a series of full papers published by our laboratory [1–6]. This subject has also been of much interest in other research groups [7–10]. Rather then republish results that are thoroughly described elsewhere, two unique themes are presented in this written contribution. The first involves an unanticipated by-product from an sp carbon-chain extension reaction. The second involves the structural characterization of monoplatinum complexes with C_6–C_8 sp carbon chains.

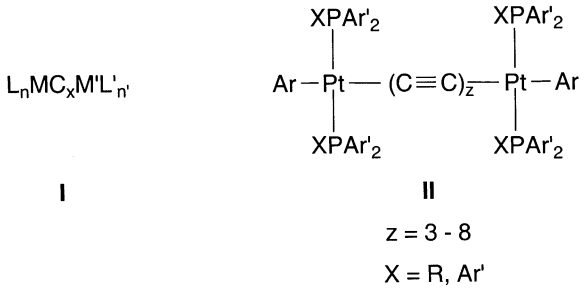

Complexes of the type **I** can exist in several valence forms (e.g., M–C, M=C, or M≡C systems) and electronic ground states (e.g., singlet/triplet). They exhibit numerous fascinating physical and chemical properties [1–10]. In many cases, interactions between the metal endgroups play key roles. In order to accurately analyse endgroup–endgroup interactions, properties of monometallic model complexes $L_nMC_xR_m$ must be precisely defined. Two recent papers provide good illustrations. The first, a collaboration with Lapinte [11], details a variety of manifestations of iron–rhenium interactions as a function of oxidation state in heterobimetallic C_4 complexes $[(\eta^5\text{-}C_5Me_5)Re(NO)(PPh_3)(C_4)(\eta^2\text{-dppe})Fe(\eta^5\text{-}C_5Me_5)]^{n+}\cdot n\ PF_6^-$ (n = 0–2). Analyses required many measurements on mono-iron and monorhenium model compounds, and the analogous di-iron and dirhenium C_4 complexes. The second is a theoretical analysis of *odd* carbon-chain complexes $[(\eta^5\text{-}C_5R_5)(NO)(PR'_3)ReC_xML_n]^{n+}$ (x = 3, 5, 7, 9), and analogous monometallic species [11]. Structural, electronic, and thermodynamic data revealed strong metal–metal interactions in some cases (ML_n = Mn/Re(CO)$_2$(η^5-C_5H_5)), but not others (ML_n = W(OMe)$_3$) [12].

We recently communicated a new series of PtC_xPt complexes (x = 8, 12, 16) with polyynediyl ($(C{\equiv}C)_n$) chains and square-planar (p-tol)(Ph_3P)$_2$Pt, (p-tol)(p-tol$_3$P)$_2$Pt, or (C_6F_5)(p-tol$_3$P)$_2$Pt endgroups, illustrated by the general structure **II** [13–16]. These are useful building blocks for more elaborate species, and are rapidly being extended, as detailed in our oral contribution. Thus, the corresponding monoplatinum complexes must also be thoroughly characterized. Accordingly, this paper reports the crystal structures of four such compounds, including one derived from an unexpected addition of the non-platinum sp terminus to acetone.

2. Results

The Hay oxidation represents one of the most useful methods for the symmetrical or cross coupling of terminal alkynes [17, 18]. An excess of O_2 and 0.20–0.25 equivalents of CuCl/TMEDA in acetone are frequently employed. As previously described [14], reaction of the readily available 1,3-butadiynyl complex *trans*-(C_6F_5)(p-tol$_3$P)$_2$PtC≡CC≡CH (**1**) and an eight-fold excess of HC≡CSiEt$_3$ under such Hay conditions gave the cross-coupled target complex *trans*-(C_6F_5)(p-tol$_3$P)$_2$PtC≡CC≡CC≡CSiEt$_3$ (**2**) in 53% yield (Fig. 1). Under standard conditions for protodesilylation [5, 6, 13], **2** was treated with n-$Bu_4N^+\ F^-$ in wet THF (0.20 equiv). The 1,3,5-hexatriynyl complex *trans*-(C_6F_5)(p-tol$_3$P)$_2$PtC≡CC≡CC≡CH (**3**) was isolated as a white powder in 85% yield after a low-temperature workup [14]. It darkened within a few minutes at room temperature, but was stable at –18 °C for several days.

The enhanced lability of longer hydrogen-capped polyynes is well documented [5, 13]. Thus, coupling conditions were sought that would allow **3** and related compounds to be used in situ. Accordingly, an acetone solution of **2** was treated with n-$Bu_4N^+\ F^-$ in wet THF to generate **3**, followed by ClSiMe$_3$ and then excess HC≡CSiEt$_3$ under the Hay coupling conditions used above [14]. Workup gave the 1,3,5,7-octatetraynyl complex *trans*-(C_6F_5)(p-tol$_3$P)$_2$PtC≡CC≡CC≡CC≡CSiEt$_3$ (**4**) in 30% yield [14]. When ClSiMe$_3$ was omitted, only traces of **4** formed. We hypothesize that fluoride ion must be scavenged prior to coupling. The yield of **4** is lowered due to the formation of some homocoupling product *trans*, *trans*-(C_6F_5)(p-tol$_3$P)$_2$PtC≡CC≡CC≡CC≡CC≡CC≡CPt(Pp-tol$_3$)$_2$(C_6F_5) (**5**). This C_{12} or dodecahexayndiyl complex is of considerable interest and use in its own right, but can be prepared in higher yield under homocoupling conditions in the absence of HC≡CSiEt$_3$ [14].

In one such sequence, SiMe$_4$ was accidentally substituted for ClSiMe$_3$. Silica gel chromatography gave a 35:65 mixture of **5** and a new species **6** (58% total). Further purification attempts were not successful. The ^{1}H NMR spectrum of the mixture showed two closely spaced $C_6H_4C\mathbf{H}_3$ signals, as well as a singlet (δ 1.53)

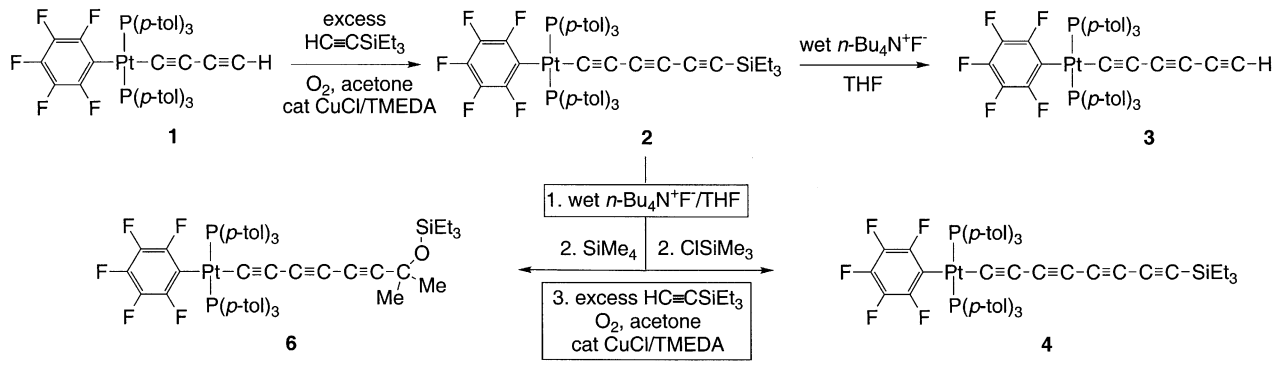

Fig. 1. Syntheses of platinum complexes.

associated with the new compound **6**. The ^{13}C NMR spectrum was not particularly informative, so the mixture was crystallized from $CHCl_3$/ethanol. The crystal structure of **5** had been previously determined [14], so a crystal of a different colour and morphology was selected in the hopes that it would correspond to the new compound **6**.

The X-ray structure was determined, and general data are summarized in Table 1. The ORTEP diagram, which shows **6** to have the structure *trans*-$(C_6F_5)(p\text{-tol}_3P)_2PtC{\equiv}CC{\equiv}CC{\equiv}CC(Me)_2OSiEt_3$, is given in Fig. 2. In a formal sense, **6** is derived from the 1,2-addition of the sp-carbon–silicon bond of **2** to acetone. However, when **2** was refluxed in acetone (45 min), no reaction occurred. Key bond lengths and angles are listed in Table 2. An ion corresponding to this mass could be found in the mass spectrum of the mixture. Furthermore, a ^{13}C NMR signal with an appropriate chemical shift and intensity for the acetone-derived methyl groups was evident (δ 32.7).

Table 1. Summary of crystallographic data.

Complex	**6**	**4**	**2**	**7**
Formula	$C_{63}H_{63}F_5OP_2PtSi$	$C_{62}H_{57}F_5P_2PtSi$	$C_{60}H_{57}F_5P_2PtSi$	$C_{55}H_{52}P_2PtSi$
Diffractometer	Nonius KappaCCD	Nonius KappaCCD	Nonius KappaCCD	Nonius KappaCCD
Temperature [K]	173(2)	173(2)	173(2)	200(0.1)
Wavelength [Å]	0.710 73	0.710 73	0.710 73	0.710 73
Crystal system	monoclinic	triclinic	triclinic	triclinic
Space group	*C*2/c	P_1	P_1	P_1
a [Å]	18.9881(2)	12.415 30(10)	12.9303(2)	12.6693(2)
b [Å]	17.9089(2)	14.2459(2)	13.2663(2)	12.8115(2)
c [Å]	34.1429(4)	17.0738(3)	15.8682(2)	17.2017(3)
α [°]	90	91.9530(4)	87.9570(10)	80.9290(9)
β [°]	95.8280(10)	95.3030(4)	88.2170(10)	80.5370(9)
γ [°]	90	109.4490(6)	89.3000(10)	60.7590(8)
V [Å^3]	11550.5(2)	2828.52(7)	2718.77(7)	2389.25(7)
Z	8	2	2	2
d_{calc} [g cm^{-3}]	1.399	1.388	1.415	1.387
Absorption coefficient [mm^{-1}]	2.562	2.612	2.715	3.063
Crystal size [mm^3]	0.20 × 0.20 × 0.02	0.30 × 0.20 × 0.15	0.30 × 0.30 × 0.10	0.31 × 0.28 × 0.10
θ limit [°]	1.20 to 26.04	1.75 to 25.01	1.28 to 27.46	1.20 to 24.39
Index ranges (*h*, *k*, *l*)	–23 to 23, –22 to 22, –42 to 42	–14 to 14, –16 to 16, –20 to 20	–16 to 16, –17 to 17, –18 to 20	0 to 14; –12 to 14; –19 to 19
Reflections collected	22 108	18 804	22 881	7816
Independent reflections	11 361 [*R*(int) = 0.0524]	9916 [*R*(int) = 0.0187]	12 290 [*R*(int) = 0.0245]	7816
Reflections [$I > 2\,\sigma(I)$]	7845	9018	10724	7491
Data/restraints/parameters	11361/0/658	9916/0/640	12290/0/622	7816/0/569
Goodness-of-fit on F^2	0.996	1.048	1.121	1.310
Final *R* indices [$I > 2\,\sigma(I)$]	*R*1 = 0.0432, *wR*2 = 0.0993	*R*1 = 0.0268, *wR*2 = 0.0637	*R*1 = 0.0260, *wR*2 = 0.0619	*R*1 = 0.0295, *wR*2 = 0.0959
R indices (all data)	*R*1 = 0.0835, *wR*2 = 0.1306	*R*1 = 0.0317, *wR*2 = 0.0660	*R*1 = 0.0355, *wR*2 = 0.0756	*R*1 = 0.063, *wR*2 = 0.1264
Δp (max), e Å^{-3}	0.919	1.175	0.614	2.515

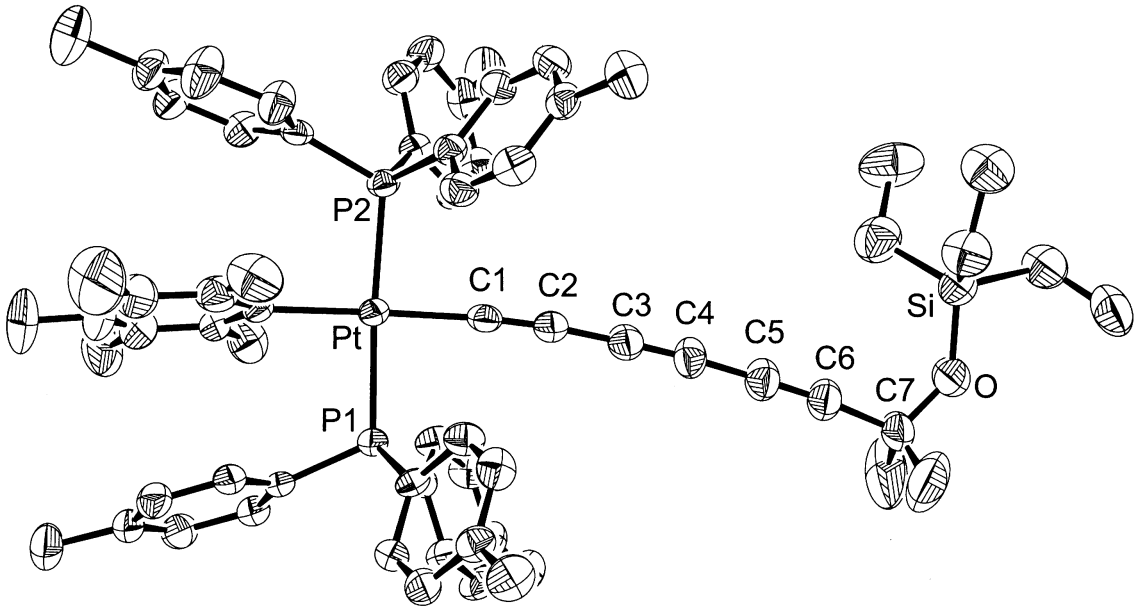

Fig. 2. Molecular Structure of *trans*-$(C_6F_5)(p\text{-tol}_3P)_2PtC{\equiv}CC{\equiv}CC{\equiv}CC(Me)_2OSiEt_3$ (**6**).

Table 2. Comparison of key bond lengths and angles.

	6	**4**	**2**	**7**
$Pt–C_1$	1.992(6)	1.986(3)	1.985(3)	2.000(5)
$C_1{\equiv}C_2$	1.206(8)	1.224(5)	1.226(4)	1.227(8)
$C_2–C_3$	1.379(9)	1.356(5)	1.362(4)	1.360(8)
$C_3{\equiv}C_4$	1.204(8)	1.219(5)	1.210(5)	1.207(9)
$C_4–C_5$	1.363(9)	1.355(5)	1.367(5)	1.369(8)
$C_5{\equiv}C_6$	1.194(8)	1.211(5)	1.206(5)	1.203(8)
$C_6–C_7$	1.483(9)	1.367(5)	—	—
$C_7{\equiv}C_8$	—	1.202(5)	—	—
$C_7–O$	1.397(8)[a]			
$C_6–Si$ or $C_8–Si$	—	1.848(4)	1.843(3)	1.835(6)
O–Si	1.636(6)	—	—	—
$Pt–P_1$	2.3085(15)	2.3044(8)	2.3111(7)	2.2963(13)
$Pt–P_2$	2.3012(15)	2.3049(8)	2.2994(7)	2.2996(14)
$Pt–C_{ipso}$	2.069(6)	2.061(3)	2.068(3)	2.079(6)
$Pt–C_1–C_2$	175.9(5)	179.3(3)	178.8(3)	176.8(5)
$C_1–C_2–C_3$	175.4(7)	177.3(4)	175.7(3)	177.0(6)
$C_2–C_3–C_4$	178.3(7)	178.4(4)	177.3(4)	178.2(6)
$C_3–C_4–C_5$	176.7(8)	175.1(4)	174.9(4)	177.2(6)
$C_4–C_5–C_6$	177.3(8)	175.7(4)	178.7(4)	178.5(7)
$C_5–C_6–C_7$	174.0(8)	174.5(4)	—	—
$C_6–C_7–C_8$	—	177.7(4)	—	—
$C_6–C_7–O$	112.6(6)			
$C_5–C_6–Si$ or $C_7–C_8–Si$	—	178.6(4)	178.8(4)	176.3(6)
$C_7–O–Si$	137.3(4)	—	—	—

[a] $C_7–Me_1$ = 1.510(12); $C_7–Me_2$ = 1.517(13).

Additional crystal structures were executed for comparison purposes. The first was that of the 1,3,5,7-octatetraynyl complex **4**, which features the same number of atoms between platinum and silicon as **6**. The second was the 1,3,5-hexatriynyl complex **2**, which contains the same number of sp-hybridised carbons as **6**. The third was the previously reported 1,3,5-hexatriynyl complex, *trans*-$(p\text{-tol})(Ph_3P)_2PtC{\equiv}CC{\equiv}CC{\equiv}CSiEt_3$ (**7**), which was obtained by a sequence analogous to that used for **2** in Fig. 1 [13]. Complexes **2** and **7** differ in the phosphine ($p\text{-tol}_3P$ vs Ph_3P) and aryl (C_6F_5 vs *p*-tol) ligands on platinum. The molecular structures are shown in Figs. 3–5, and other data are incorporated into Tables 1 and 2.

3. Discussion

All of the structurally characterized complexes feature PtC≡CC≡CC≡C linkages. Complexes with 1,3-butadiynyl ligands have recently been comprehensively reviewed by Low and Bruce [19], and crystal structures of several platinum adducts have been reported. To our knowledge, no higher monoplatinum polyynyl species have been structurally characterized, as verified by an independent search of the Cambridge database. However, the crystal structures of a number of diplatinum complexes of the type **II** have been determined [13, 14, 20]. Crystallographic data and packing motifs for conjugated octatetraynes with both organic and transition metal endgroups are summarized in detail elsewhere [21].

Turning to the data in Table 2 and Figs. 2–5, the C_8 chain in octatetraynyl complex **4** shows a slight but distinct bending. The average bond angle, 177.1°, is not very different from 180°, but the deviations are complementary and reinforce the curvature. The platinum–silicon distance, 12.6168(10) Å, is 1% shorter

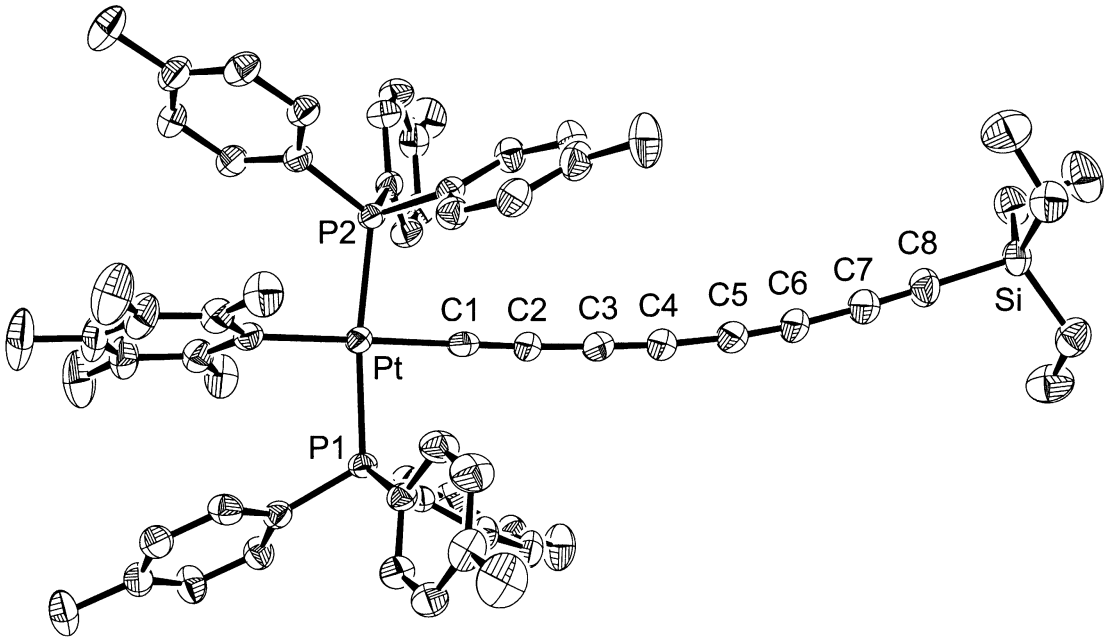

Fig. 3. Molecular structure of *trans*-$(C_6F_5)(p\text{-tol}_3P)_2PtC{\equiv}CC{\equiv}CC{\equiv}CC{\equiv}CSiEt_3$ (**4**).

than the sum of the nine intervening bond lengths, 12.768 Å. By these criteria, **4** is similar to several other tetraynes, including $(\eta^5\text{-}C_5Me_5)Re(NO)(PPh_3)(C{\equiv}CC{\equiv}CC{\equiv}CC{\equiv}CSiMe_3)$ [21] and one with cyclobutadienyl cobalt endgroups (average angles 177.5°, 176.7°) [22]. One tetrayne, $(\eta^5\text{-}C_5Me_5)Re(NO)(PPh_3)(C{\equiv}CC{\equiv}CC{\equiv}CC{\equiv}C\text{-}p\text{-tol})$ [23], exhibits distinctly greater bending (average angle 175.7°). The hexatriynyl complexes **6**, **2**, and **7** have average bond angles of 176.3°, 177.4°, and 177.3°, but since there are fewer sp carbons the bending (Figs. 2, 4 and 5) is not as visually dramatic.

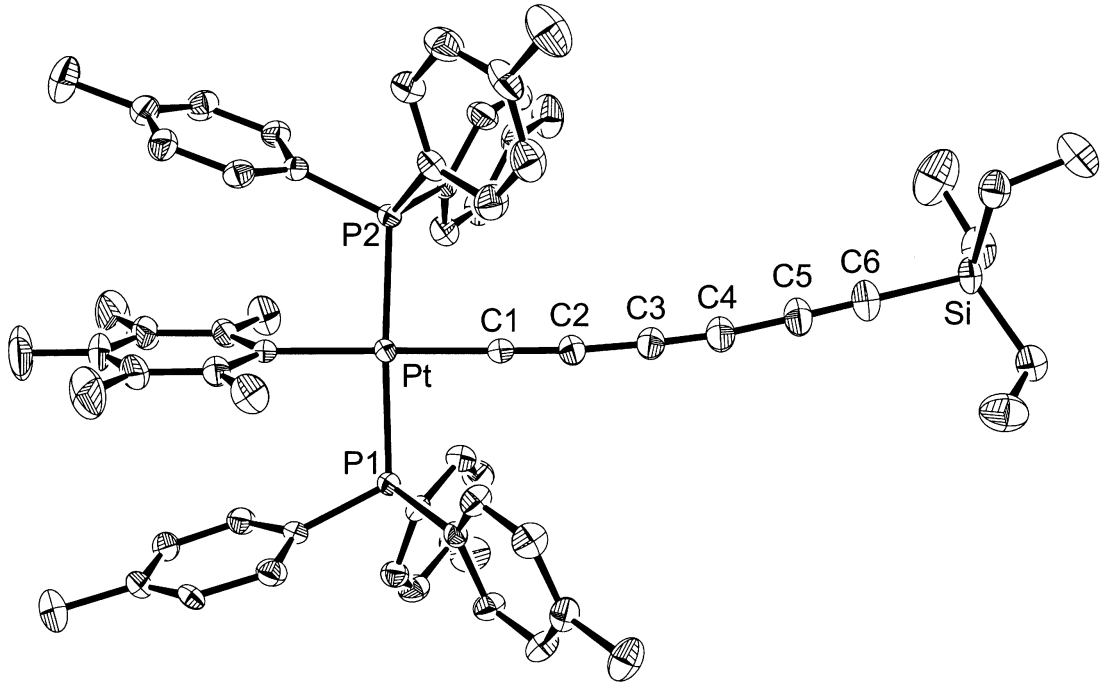

Fig. 4. Molecular structure of *trans*-$(C_6F_5)(p\text{-tol}_3P)_2PtC{\equiv}CC{\equiv}CC{\equiv}CSiEt_3$ (**2**).

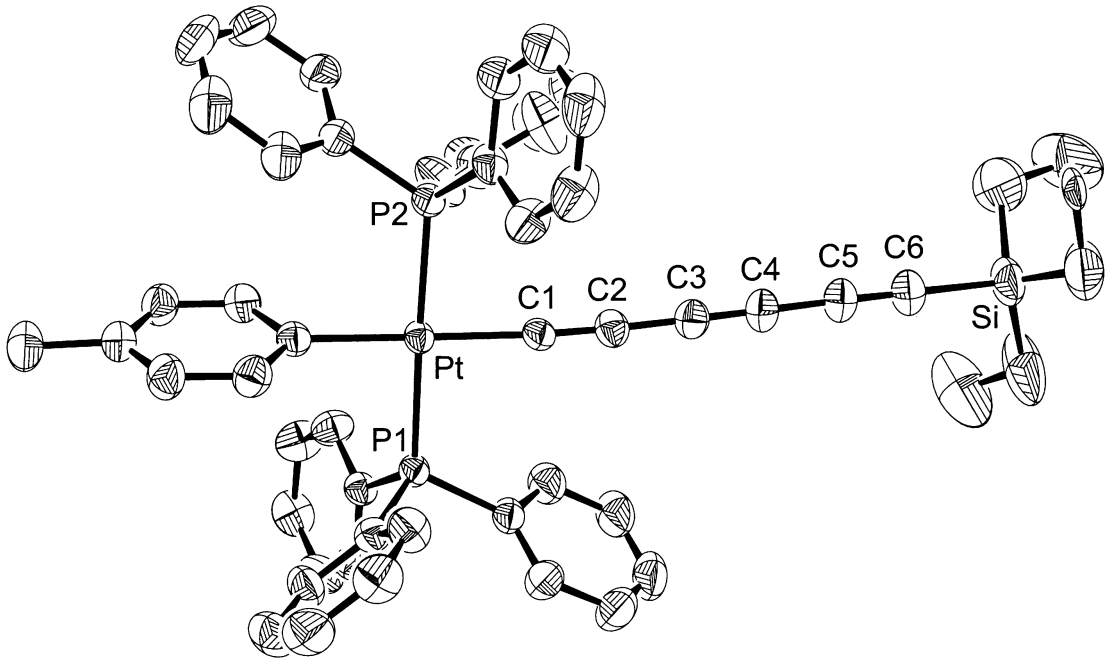

Fig. 5. Molecular structure of *trans*-(*p*-tol)$(Ph_3P)_2$PtC≡CC≡CC≡C$SiEt_3$ (**7**).

The Pt–C≡C–C≡C–C≡C bond lengths in homologous complexes **4** and **2** are identical within experimental error. The Pt–C_{ipso} bond lengths and the average of the two Pt–P bond lengths are also identical. Only one or two bond angles show meaningful differences. Furthermore, the space groups are identical, and the unit cells show analogous packing motifs. Somewhat greater bond length and angle differences are evident in **6**. Of these, the Pt–C≡C angles are the most noteworthy. The M–C≡C linkages are often among the most bent in the chain, presumably reflecting their lower bending force constants (vs C–C≡C). The angle in **6** (175.9(5)°) is typical. However, **4** and **2** exhibit nearly linear linkages (179.3(3)°, 178.8(3)°). Some of the bond lengths and angles of **7** lie at the extremes of the other compounds, but the differences are not great enough for a distinct endgroup effect to be claimed. In all four compounds, the aryl ligands adopt similar Pt–C_{ipso} conformations, with angles of 73.8°–76.7° between the least squares planes of the aryl ring and platinum (P1–Pt–C_{ipso}–C_{ortho}; **6**/**4**/**2**/**7** 76.7°/73.8°/74.8°/74.3°).

The following points are relevant to the formation of **6**. First, additions of silicon compounds of the type $XSiR_3$ to carbonyl groups are well known, and can in many cases be catalysed by nucleophiles. The fluoride ion-mediated addition of HC≡C$SiMe_3$ to carbonyl compounds has been explicitly reported [24]. An anionic PtC≡CC≡CC≡C$^-$ species would likely be generated when **2** is treated with *n*-Bu_4N^+ F^- in wet THF (Fig. 1), both in the initial step and then in small equilibrium amounts from the protonation product **3**. Curiously, the IR monitoring of several reactions like these has established that only substoichiometric quantities of *n*-Bu_4N^+ F^- are needed. Following acetone addition, a triethylsilyl group could be transferred from the eight-fold excess of HC≡C$SiEt_3$ or from the other $XSiEt_3$ species present. However, what would exactly inhibit acetone addition/silylation under the conditions involving $ClSiMe_3$, or promote addition/silylation under the conditions utilizing $SiMe_4$, is a matter of speculation. There are simply too many variables, and narrowing the possibilities would require an extensive series of control experiments. For obvious reasons, we wish to avoid a lengthy formal mechanistic study of an unwanted side reaction.

With regard to future research with compounds of the types **I** and **II**, chain lengthening will be an important theme. There is no doubt that compounds with very long sp carbon chains have been generated in solution. These include a C_{32} hexadecayne with SiR_3 endgroups [25], and a C_{24} dodecayne with *t*-butyl endgroups [26]. The question that should be answered shortly is whether transition metal endgroups, which are electropositive and commonly quite bulky, will enhance stabilities and allow such compounds to be isolated and thoroughly characterised. The current records stand at C_{20} for the (η^5-C_5Me_5)Re(NO)(PPh_3) endgroup [4], and C_{16} for the (C_6F_5)(*p*-tol_3P)$_2$Pt endgroup [14]. In all of these efforts, the physical and chemical study of monome

tallic model compounds, as exemplified by the structural and reactivity data in this paper, will play an essential role [27].

4. Experimental

For the general procedures employed, see references [13–16].

4.1. Synthesis of 6

A three-necked flask was charged with **2** [14] (0.201 g, 0.174 mmol) and acetone (15 ml), and fitted with a gas dispersion tube and a condenser. A Schlenk flask was charged with CuCl (0.100 g, 1.02 mmol) and acetone (30 ml), and TMEDA (0.060 ml, 0.40 mmol) was added with stirring. After 30 min, stirring was halted and a green solid separated from the blue supernatant. Then n-$Bu_4N^+ F^-$ (1.0 M in THF/5 wt% H_2O, 0.040 ml, 0.040 mmol) was added to the solution of **2** with stirring. After 10 min, $SiMe_4$ (0.014 ml, 0.103 mmol) was added. After 20 min, the condenser was cooled to –20 °C. Then O_2 was bubbled through the three-necked flask, and the solution was heated to 65 °C. After ca 10 min, $HC{\equiv}CSiEt_3$ (0.197 g, 1.404 mmol) was added, followed by portions of the blue supernatant. After 3 h, solvent was removed by rotary evaporation. The residue was extracted with hexane (3 × 5 ml) and then benzene (3 × 5 ml). The extracts were passed in sequence through an alumina column (15 cm). Solvent was removed from the benzene extracts by rotary evaporation and oil pump vacuum. The resulting yellow powder was chromatographed on a silica gel column (15 cm) with 10:90 v/v CH_2Cl_2/hexane to elute traces of **4** [6] and then 40:60 v/v CH_2Cl_2/hexane to elute a second band. The latter was taken to dryness by oil pump vacuum to give a yellow powder that was a 65:35 mixture of **6** and **5** (0.114 g, 0.049/0.026 mmol, 28%/30%), as assayed by ^{1}H NMR.

IR (cm^{-1}, powder film) $\nu_{C{\equiv}C}$ 2150 (s), 2038 (m), and bands of **5** [14]. NMR (δ, $CDCl_3$, signals of **5** [14] omitted unless noted): ^{1}H 7.45 (m, 12H, *o* to P), 7.10 (d, $^3J_{HH}$ = 7.4 Hz, 12H, *m* to P), 2.35 (s, 18H, $C_6H_4CH_3$), 1.53 (s, 6H, $C(CH_3)_2O$), 0.87 (t, $^3J_{HH}$ = 7.8 Hz, 9H, CH_2CH_3), 0.59 (q, $^3J_{HH}$ = 7.8 Hz, 6H, CH_2CH_3); $^{13}C\{^1H\}$ (partial; the signals *o*/*m*/*p* to Pt are very close to those of **5** and $^1J_{CF}$ and $^2J_{CF}$ values could not be determined) 145.2 (dd, *o* to Pt), 140.3 (s, *p* to P), 136.9 (dm, *p* to Pt), 136.2 (dm, *m* to Pt), 140.3 (s, *p* to P), 133.8 (virtual t, $^2J_{CP}$ = 6.5 Hz, *o* to P), 128.3 (virtual t, $^3J_{CP}$ = 5.5 Hz, *m* to P), 127.1 (virtual t, $^1J_{CP}$ = 30.2 Hz, *i* to P), 95.5, 79.7, 69.7, 68.2, 66.3, 65.8, 63.1, 61.0, 57.2 (9 s, C≡ of **6** and **5**), 54.9 (s, **C**$(CH_3)_2O$, tentative), 32.7 (s, **C**$(CH_3)_2O$), 21.1 (s, $C_6H_4CH_3$), 6.7 (s, CH_2CH_3), 5.7 (s, CH_2CH_3); $^{31}P\{^1H\}$, 17.9 (s). MS (*m*/*z*; FAB, 3-NBA) 1215 (**6**-H$^+$, 10%), 970 ($[(C_6F_5)Pt(Ptol_3)_2]^+$, 50%), 802 ($[Pt(Ptol_3)_2–H]^+$, 50%).

4.2. Crystallography

A $CHCl_3$ solution of **6** and **5** (65:35) was layered with ethanol. After 14 h at room temperature, a mixture of thin colourless plates (**6**) and yellow powder (**5**) had formed. One of the former was removed and data were collected as outlined in Table 1. Cell parameters were obtained from 10 frames using a 10° scan and refined with 11 450 reflections. Lorentz, polarisation, and absorption corrections [28, 29] were applied. The space group was determined from systematic absences and subsequent least-squares refinement. The structure was solved by direct methods. The parameters were refined with all data by full-matrix-least-squares on F^2 using SHELXL-97 [30]. Non-hydrogen atoms were refined with anisotropically. The hydrogen atoms were fixed in idealized positions using a riding model. Scattering factors were taken from the literature [31].

A $CHCl_3$ solution of **4** was slowly concentrated by evaporation. After several days at room temperature, one of the yellow needles was removed. A CH_2Cl_2 solution of **2** was layered with ethanol. After several days at room temperature, a yellow needle was removed. Data were collected and the structures refined and solved exactly as for **6**.

A concentrated CH_2Cl_2 solution of **7** [13] was layered with hexanes and slowly concentrated by evaporation. After two weeks, a colourless needle was removed, and data were collected as outlined in Table 1. Cell parameters were obtained from 10 frames using a 10° scan. The space group was determined from least-squares refinement. Lorentz, polarisation and absorption corrections were applied using DENZO-SMN and SCALEPACK [29]. The structure was solved by standard heavy atom techniques with the SIR97 package and refined with SHELXL-97 [30]. Non-hydrogen atoms were refined with anisotropic thermal parameters. Two ethyl groups showed displacement disorder (C81/C81', C82/C82', C83/C83', C84/C84'), which could be solved and refined to a 77:23 ratio. Hydrogen atom positions were calculated and added to the structure factor calculations, using the riding model. Scattering factors, as well as $\Delta f'$ and $\Delta f''$ values, were taken from literature [32, 33].

. Supplementary material

All crystallographic data (excluding structure factors) have been deposited with the Cambridge Crystal

lographic Data Centre, CCDC nos. 166712 (**6**), 166711 (**4**), 166710 (**2**), and 134398 (**7**). Copies of this information can be obtained free on application to CCDC, 12 Union Road, Cambridge CB2 1EZ, UK. [Fax: (internat.) + 44-1223/336-033; E-mail: deposit@ccdc.cam.ac.uk].

Acknowledgements. We thank the Deutsche Forschungsgemeinschaft (DFG, GL 300/1-1) and Johnson Matthey PMC (platinum loan) for support of this research.

References

[1] Weng W., Bartik T., Brady M., Bartik B., Ramsden J.A., Arif A.M., Gladysz J.A., J. Am. Chem. Soc. 117 (1995) 11922.

[2] Brady M., Weng W., Zhou Y., Seyler J.W., Amoroso A.J., Arif A.M., Böhme M., Frenking G., Gladysz J.A., J. Am. Chem. Soc. 119 (1997) 775.

[3] Falloon S.B., Szafert S., Arif A.M., Gladysz J.A., Chem. Eur. J. 4 (1998) 1033.

[4] Bartik T., Weng W., Ramsden J.A., Szafert S., Falloon S.B., Arif A.M., Gladysz J.A., J. Am. Chem. Soc. 120 (1998) 11071.

[5] Dembinski R., Bartik T., Bartik B., Jaeger M., Gladysz J.A., J. Am. Chem. Soc. 122 (2000) 810.

[6] Meyer W.E., Amoroso A.J., Horn C.R., Jaeger M., Gladysz J.A., Organometallics 20 (2001) 1115.

[7] Bruce M.I., Coord. Chem. Rev. 166 (1997) 91.

[8] Paul F., Lapinte C., Coord. Chem. Rev 431 (1998) 178–180.

[9] Sakurai A., Akita M., Moro-oka Y., Organometallics 18 (1999) 3241.

[10] Fernández F.J., Blacque O., Alfonso M., Berke H., J. Chem. Soc., Chem. Commun. (2001) 1266 and references therein.

[11] Paul F., Meyer W.E., Toupet L., Jiao H., Gladysz J.A., Lapinte C., J. Am. Chem. Soc. 122 (2000) 9405.

[12] Jiao H., Gladysz J.A., New J. Chem. 25 (2001) 551.

[13] Peters T.B., Bohling J.C., Arif A.M., Gladysz J.A., Organometallics 18 (1999) 3261.

[14] Mohr W., Stahl J., Hampel F., Gladysz J.A., Inorg. Chem. 40 (2001) 3263.

[15] Bohling J.C., Peters T.B., Arif A.M., Hampel F., Gladysz J.A., in: Ondrejoviç G., Sirota A. (Eds.), Coordination Chemistry at the Turn of the Century, Slovak Technical University Press, Bratislava, Slovokia, 1999.

[16] Peters T.B., Zheng Q., Bohling J.C., Arif A.M, Gladysz J.A., J. Organomet. Chem. 641 (2001) 53.

[17] Siemsen P., Livingston R.C., Diederich F., Angew. Chem., Int. Ed. Engl. 39 (2000) 2633.

[18] Siemsen P., Livingston R.C., Diederich F., Angew. Chem. 112 (2000) 2740.

[19] Low P.J., Bruce M.I., Adv. Organomet. Chem. 48 (2001) 71.

[20] Stahl J., Bauer E., Hampel F., Universität Erlangen-Nürnberg, unpublished results.

[21] Bartik B., Dembinski R., Bartik T., Arif A.M., Gladysz J.A., New J. Chem. 21 (1997) 739.

[22] Altmann M., Enkelmann V., Bunz U.H.F., Chem. Ber. 129 (1996) 269.

[23] Dembinski R., Lis T., Szafert S., Mayne C.L., Bartik T., Gladysz J.A., J. Organomet. Chem. 578 (1999) 229.

[24] Abele E., Rubina K., Abele R., Popelis J., Mazeika I., Lukevics E., J. Organomet. Chem. 586 (1999) 184 and references therein.

[25] Eastmond R., Johnson T.R., Walton D.R.M., Tetrahedron 28 (1972) 4601.

[26] Jones E.R.H., Lee H.H., Whiting M.C., J. Chem. Soc. (1960) 3483.

[27] Johnson T.R., Walton D.R.M., Tetrahedron 28 (1972) 5221.

[28] 'Collect' data collection software, Nonius B.V., 1998.

[29] 'Scalepack' data processing software: Z. Otwinowski, W. Minor, Macromol. Crystallogr. A 276 (1997) 307.

[30] Sheldrick G.M., SHELX-97, Program for refinement of crystal structures, University of Göttingen, 1997.

[31] Cromer D.T., Waber J.T., in: Ibers J.A., Hamilton W.C. (Eds.), International Tables for X-ray Crystallography, Kynoch, Birmingham, England, 1974.

[32] Maslen E.N., Fox A.G., O'Keefe M.A., in: Wilson A.J.C. (Ed.), International Tables for Crystallography: Mathematical, Physical and Chemical Tables, Vol. C, Chapter 6, Kluwer, Dordrecht, The Netherlands, 1992, pp. 476–516.

[33] Creagh D.C., McAuley W.J., in: Wilson A.J.C. (Ed.), International Tables for Crystallography: Mathematical, Physical and Chemical Tables, Vol. C, Chapter 4, Kluwer, Dordrecht, The Netherlands, 1992, pp. 206–222.